Thermal hysteresis of mesoscopic phase transitions in fluid metals: from tantalum to aluminum and gold with their critical points and non-mean-field global diagrams

O. V. Rogankov (oleg.rogankov@gmail.com)
G. S. Dragan
Physics Research Institute Odesa I. I. Mechnikov National University
V. B. Rogankov
Physics Research Institute Odesa I. I. Mechnikov National University

Research Article

Keywords: dynamic irreversibility, mesoscopic, subsecond thermophysical properties, aluminum, gold congruent phase diagram, FT-calibration, IEX-temperature

Posted Date: September 29th, 2022

DOI: https://doi.org/10.21203/rs.3.rs-2099925/v1

Thermal hysteresis of mesoscopic phase transitions in fluid metals: from tantalum to aluminum and gold with their critical points and non-mean-field global diagrams

O.V. Rogankov, G.S. Dragan, V.B. Rogankov

0000-0002-1559-4548 0000-0002-3626-9760 0000-0002-5230-3340

Physics Research Institute Odesa I. I. Mechnikov National University, Ukraine

oleg.rogankov@gmail.com

Abstract

The light *soft* metal – Al-IIIB ($M^{\mathrm{Al}}=27\ \mathrm{g\cdot mol^{-1}}$) and the heavy *soft* metal – Au-IB ($M^{\mathrm{Au}}=197\ \mathrm{g\cdot mol^{-1}}$) were analyzed within the same predictive model of fluctuation–thermodynamics (FT). The similar extrapolative approach was applied for re-establishing of the global phase diagram and non-mean-field criticality of the refractory heavy and *rigid* tantalum Ta-VA ($M^{\mathrm{Ta}}=181\ \mathrm{g\cdot mol^{-1}}$) earlier. The revealed then correspondence between the onset point of nano-droplets at atmospheric pressure and the point of instability, observable at much higher pressures by the dynamic (IEX) measurements, found its confirmation for the considered metals as well. It may indicate the universality of the mentioned "dew"-point for any elements and compounds. The mesoscopic nanoscaled time- and length- simultaneous consideration matters especially for all metallic vapors at sub-atmospheric pressures ($P<P_0$) and $T<T_b$. The FT-predicted critical points of Al $\left\{T_c^{\mathrm{Al}}=6518\ \mathrm{K};\ \ \rho_c^{\mathrm{Al}}=424.5\ \mathrm{kg\cdot m^{-3}};\ \ P_c^{\mathrm{Al}}=1369\ \mathrm{bar};\ \ Z_c^{\mathrm{Al}}=0.1607\right\}$ and Au $\left\{T_c^{\mathrm{Au}}=8077\ \mathrm{K};\ \ \rho_c^{\mathrm{Au}}=3453\ \mathrm{kg\cdot m^{-3}};\ \ P_c^{\mathrm{Au}}=2135\ \mathrm{bar};\ \ Z_c^{\mathrm{Au}}=0.1814\right\}$ are consistent with the available low-temperature thermostatic and rapid dynamic experimental data.

Key words: dynamic irreversibility, mesoscopic, subsecond thermophysical properties, aluminum, gold congruent phase diagram, FT-calibration, IEX-temperature.

All authors contributed to the study conception and design. Material preparation, data collection and analysis were performed by Vitaly B. Rogankov, Grygorii S. Dragan and Oleg V. Rogankov. The first draft of the manuscript was written by Vitaly B. Rogankov and all authors commented on previous versions of the manuscript. All authors read and approved the final manuscript.

1.Introduction

The thermodynamically consistent unification of the high-temperature two-phase thermophysical properties, for refractory metals is invaluable in many applications. This problem includes: (*i*) – the development of adequate theoretical model with the optimum number of physically – meaningful input parameters; (*ii*) – the well-established extrapolation procedure to transform the limited experimental data into the description of the high-pressure-temperature regions including criticality and metastability; (*iii*) – the reasonable consistency of, atomistic by nature, MD-simulated on picosecond time- and nanometer length-scales properties with the available experimental data of subsecond IEX-measurements. The latters are usually performed on the microsecond scale of time and the milimetre scale of length for the electrically conductive refractory metals. The applied here FT-model has been already implemented successfully for alkali and alkaline-earth metals [2,3] as well as for two families of the heavier isotopes for water [4] and methane [5], polar methanol [2], several inert gases and ionic liquids [6].

This work follows the study of the non-mean-field congruent vapor-liquid (CVL) phase diagram for Ta in [1], where the FT-predictive scheme was described in detail. Thus, now we will refer to some equations of it to avoid the unnecessary repetition, while the basic FT-correlations for the current work will be considered directly in the context. The formulated concept of mesoscopic irreversibility questions not the experimental IEX-data themselves, but their thermostatic locally-equilibrium (LE) – interpretation. For readers not yet familiar with the set of dynamic ultrafast techniques [7-14] including the accepted fit of thermophysical data, the seminal consideration of relevant tasks and limitations reported in [9,10] could be useful. The problem of the magneto-hydrodynamic (*mhd*) – instability manifested by the sharp growth of electrical resistivity and the concomitant too high specific heat capacity for transition metals $\left(C_P M \approx 6 \text{ to } 7R \text{ for Ta}\right)$ was posed long ago and remains unsolvable until now. Besides, the consistency of reported

static measurements of Al [15] for example, with its fast dynamic IEX-experiments [13] needs a refinement even in the close vicinity of melting T_m – point.

We have supposed that the combination of the hydrodynamic balance equations with the mean-field theory of a phase transition [16,17] can lead to the principle mistakes. Especially it concerns the usual ideal-gas modeling of heterogeneous metallic vapor. The concept of the unified, common for both coexistent fluid *f*-phases (*f* = *g* or *l*) EOS, used for an explanation of *mhd*-instability [9-12,16] may be the potential source of resultant inadequacy. The continuous reversible infinitely-slow isothermal transformation itself applied to both macroscopic finite-volume *f*-phases is unrealizable by any practical finite-time measurements. Vaporization of the, locally ordered, condensed bulk matter [18-24] into the supposedly homogeneous disordered gaseous *g*-state, starts from the explosive-like destruction of *l*-homogeneity. The direction-dependent rate of transition and its irreversibility is a more reasonable assumption for the non-mean-field consideration. At the coupled *destructive* process of vaporization and the inverse *constructive* process of condensation the excess disbalanced heat should be emitted. The dubious validity of the thermostatic equal areas rule symbolizing the idealized reversibility, provides a qualitative binodal – image of the actual coexistent curve in the (T,ρ)–plane; $\{\rho_g(T),\rho_l(T)\}$. This construction can "mask" any EOS-induced inaccuracy of chemical *f*-potentials if the adjusting prescribed equality: $\mu_g(T)=\mu_l(T)$ becomes fulfilled.

The experienced upper limit of the "working temperature window" in IEX-experiments $(T_{mhd}-T_m)$ for liquids is always located above or nearly to the high temperatures of normal boiling point $T_b(\rho_l,P_0)$ for many metals [9]. The proposed option of congruent CVL-predictions [1-6] is realizable just in the respective long "low-temperature" interval for sub-atmospheric vapor pressures: $P_v(T\le T_b)=P_0$. For metals this vacuum is located far beyond the scope of predictive capability for the typical unified semi-empirical *mf*-EOS [23-29]. One of the apparent reasons for

such failure is often noted at the discussion of IEX-data [7-14]. Its purpose is to explain the negligible effect of pressure-related deviations in density $\rho_l(T)$. Their irrelevance is explainable by the extremely low isothermal compressibility β_T of liquid metals. Nevertheless, the singular and infinite mean-field "jump" of compressibility at the stable points of *binodal* from about zero $\beta_T(T, P_v \to 0) \to 0$ to infinity: $\beta_T(T, P_v) \to \infty$ is questionable in a finite volume. The supposedly enormous negative pressures $P = 0$ of the metastable *ml*-points at low temperatures $T = T_b$ also seem like fictitious consequences of the aforementioned inadequacy in the real finite-time, finite-volume fluid *f*-system.

In Section 2 the general features of the alternative non-mean-field origin of *mhd*-instability inserted into the conventional IEX-formalism are outlined. They are termed by us as the method of *FT-calibration*. In Section 3 the critical points and the CVL- diagrams for aluminum and gold are predicted. Both end-points of a reference Eq.(1) from the work [1], belong to the *imaginable straight line* identified with the scaling FT-model's P_0-isobar. It can be obtained by the extrapolation to both axes $(\rho = 0, T = 0)$ of the relatively short linear *l*-segment. The latter follows from an actual atmospheric isobar measurable for Al and Au at $P_0 = 0.1\,\text{MPa}$. The discovered by FT-model non-mean-field *significant shrinking of the metastable liquid (ml) area* for Al and Au in the $(T, \rho)-$projection is very informative. Its shape is qualitatively comparable with that following from the extrapolation into two-phase region of the supercritical *f*-phase simulated results obtained along the *ideal curves* of molecular fluids SF_6, CO_2 and H_2O [28]. The term of *ideal curves* was introduced by V.I. Nedostup [25] and used then as the Zeno-line by many others [26-29]. Unfortunately, this outstanding scientist past away recently. The performed in Section 4 comparative analysis of *FT-calibration* applied to Ta [1] and to Al here demonstrates the promising predictive capability of CVL-diagram for the explanation of *mhd*-instability. The specific peculiarities of the proposed FT-calibration is described in Section 4 in the context of

comparative investigation of the binding and cohesive energies. This problem is often discussable in the thermophysical handbooks and different PCS- correlations for liquid metals [30-33].

2. The knot of FT calibration – the key lines of a mesoscopic CVL – diagram

The electrical conductivity: $\sigma_e = \rho_e^{-1}(h)$ or resistivity at the expansion of the specific volume $v_l(h)/v_s(T_s)$ are mutually measurable by the subsecond dynamic experiments in a condensed matter versus enthalpy. Its unquestionably non-equilibrium value $h_l(t)$ is expressible by the supposedly isobaric integral form for specific (per unit of mass) enthalpy [9,11]. This quantity corresponds to the differential Joule-Lentz's heat in Eq.(36) from [1]. The natural consequence of both equivalent Horstamann's and Clausius' expressions of the Second Law was used for the concept of IEX-irreversibility introduction. It means that an actual dynamic process should be sooner a polytropic pathway with the finite heat capacity functional of temperature dependent on specific entropy $C_{JL}\{T(s)\}$ [1] than the isobaric one with its thermostatic function $C_P(T)$. The preferable at the study of IEX experiments Horstmann's form (8a) in [1] implies that the energy content of sample during the state change $\Delta t-$ interval can be determined without any ambiguity through the changeable volume v_l (or density $\rho_l = 1/v_l$) and temperature T_l. Hence, the consumed from the external source integral heat quantity δh_{JL} and its rate in Eq.(36[1]) is irrespective of what are the ways of $T-$ change with $\Delta T/\Delta t-$ rate and the physical source of input heat. The necessity of the coherent FT-calibration for the determinative changes of $v_l = \rho_l^{-1}(t)$ and $T_l(s_l)$, as a polytrophic function of entropy according to the Clausius form Eq.(8b[1]), becomes obvious. The required *synchronization* of the continuous $T(t)-$ function with the input *measurable non-equilibrium enthalpy* $h_{JL}(t)$ seems to be the most subtle and serious underlying problem of the proposed FT-

calibration. The usually admissible elimination of time *t* from the set of IEX-data can imply the reach of LE-state in a single experimental shot indeed [9] only after its appropriate performance.

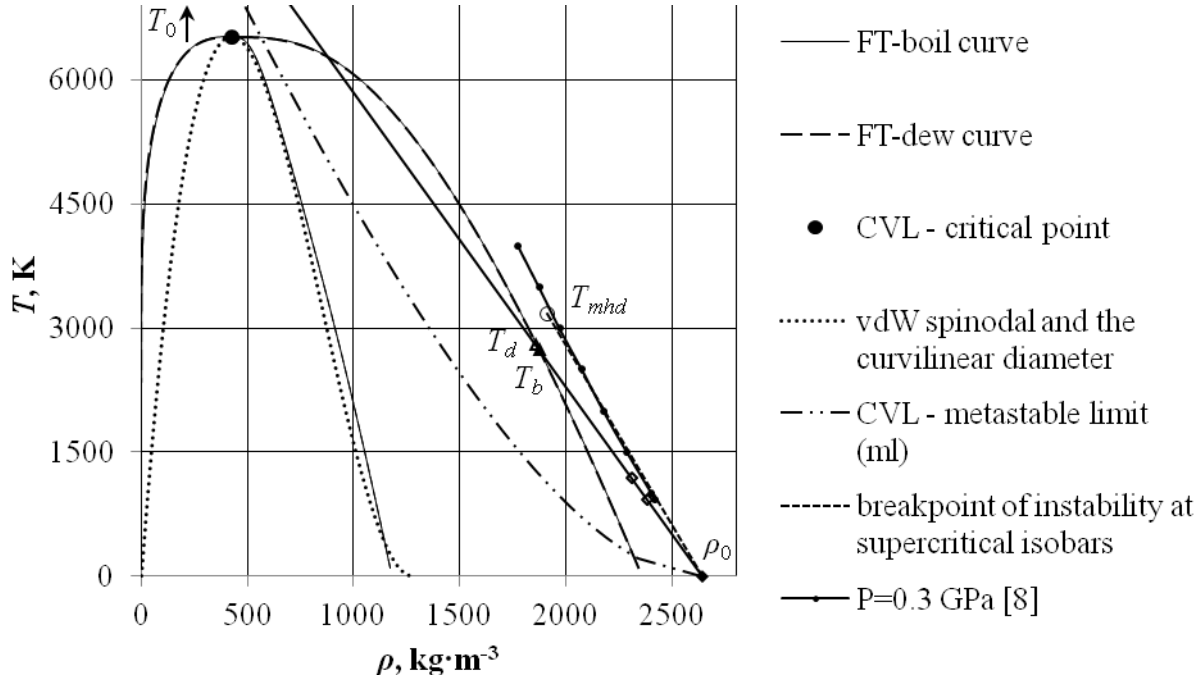

Fig.1 Global CVL – phase diagram for Al with critical point $\{T_c = 6518\,K$; $\rho_c = 424.5\,\mathrm{kg\cdot m^{-3}}$ and $P_c = 1369$ bar, $\lambda = 1/Z_c = 6.2\}$ elucidates the problem of mhd – instability posed by Gathers [8,9]. It is evident that: a) – the IEX – isobar $P = 3000\,\mathrm{bar} > P_c$ is concave everywhere (non-congruent as *ml*-limit of CVL – metastability is); b) – the experimentally observable liquid mhd – instability "starts" at the breakpoint T_{mhd} located above T_d *where the inequality* $1/Z \geq \lambda$ *becomes fulfilled in the compressed state*. For the input P_0 – isobar [15] with the changed slope only two points ($T_m = 933.2$ K, $\rho_m = 2380\,\mathrm{kg\cdot m^{-3}}$) [24] and $\left(T = 1190\,\mathrm{K},\ \rho = 2308\,\mathrm{kg\cdot m^{-3}}\right)$ are shown by two diamonds. $T_0^{\mathrm{Al}} = 9426$ K lies outside the region shown. The mean-field spinodal is represented here to illustrate its irrelevance to the *mhd*-problem

In total, our results for Ta shown in the $(T,\rho)-$ plane of Fig.1[1] correspond to the above expectation but with one rather annoying exclusion. It concerns the unacceptably large systematic discrepancy between two sets of experimental data reported in [7] and [14]. The mean-field concept of a unified soft sphere EOS was used by Young [24] in the context of its van der Waals' modification [23]. The deviation of [7] from [14] varies from 3.8% at $T_m = 3280$ K

up to 18.8% at $T_{mhd} = 7400\,\mathrm{K} \approx T_d = 7472\,\mathrm{K}$. Thus the $T_{mhd} -$ value was reliably estimated by the temperature $\left(T_d - T_b\right) -$ width of $v -$ interphase in CVL-diagram [1]. At first sight, one should simply disavow the older data because of the reported densities which imply the negative modulus of mechanical instability: $1/\beta_T < 0$. While measured at very high pressures: $P = 0.1; 0.2; 0.3\,\mathrm{GPa}$ [7,24] they were significantly lower than densities measured in [14] at about atmospheric pressure $P = 0.23\,\mathrm{MPa}$ and the equal temperatures. The low-pressure measured $\rho(T) -$ data [14] were selected by us as the acceptable approximation for the reference atmospheric isobar $P_0 = 0.1\,\mathrm{MPa}$ described by Eqs. (1,2) in [1].

We state now that *both sets of the different IEX-measurements for Ta are still compatible* (see Section 4) *within the experimental uncertainty of density* ($< 2.5\%$). The drastic change of IEX-interpretation can be argued in the framework of proposed below non-mean-field FT-calibration. It will be applied to the original Gathers' data for Ta [7] and Al [8]. To gain such aim let us remind that FT-model and its CVL-diagram predict independently the existence of a mesoscopic heterogeneous $v -$ interphase [2 – 6]. This well-established result postulates the presence of neighboring *b*- and *d*- branches on the CVL-projections at the description of mesoscopic *l*- states. Moreover, the following distinctive features of the universal FT-consideration are noticeable. It is applicable to any (not only metallic) elements and isotopes as well as to any molecular compounds and their isotopes. The determinative quantity for mechanical stability of a condensed matter in FT-model is the scale-invariant and *T-independent binding energy* $e^{FT}_{bind\,f}$. It connects locally the neighboring constituent particles for a substance at any external $(T, P)-$conditions. FT-model expresses this factor in terms of the one-atom effective FT-potential $\phi^{FT}\left(r; \varepsilon^{FT}, \sigma_f^{FT}, r_f^{FT} \geq r; n/6\right)$ unusual for metals, attributed to the specific *f*-phase:

$$\varepsilon^{FT} = kT_c\left(1 - Z_c\right) = kT_c - P_c/n_c \qquad (1)$$

$$\sigma_f^{FT} = \left\{ 3\left(Ri^f - 2 \right) \Big/ \left[4\pi n_c \left(Ri^f - 1 \right) \right] \right\}^{1/3} \tag{2}$$

$$\lambda^{FT} = r_f \Big/ \sigma_f^{FT} = 1/Z_c = T_c^* \Big/ \left(T_c^* - 1 \right) \tag{3}$$

$$e_{bind\,f}^{FT} = \frac{\lambda_e \varepsilon^{FT}}{m_n \sigma_f^{FT}} \left(\frac{\rho_{nf}}{\rho_c} \right)^3 = \frac{h\varepsilon^{FT}}{m_e c m_n \sigma_f^{FT}} \left(\frac{\rho_{nf}}{\rho_c} \right)^3 \tag{4}$$

Here m_n corresponds approximately to the nucleon mass, $\rho_{nf} = 6m_n \Big/ \left(\pi \sigma_f^3 \right)$ – is its density in a supposedly spherical volume. The electron wavelength: $\lambda_e = h \Big/ \left(m_e c \right)$; 2.43 pm is expressed as usually via the Planck's constant *h,* mass of electron m_e and the velocity of light in vacuum *c*. The given $\lambda_e -$ value determines in Eq.(4) the universal limit of a continuous consideration applied to the discrete atomistic (nucleon) structure admissible by FT-model. The next coupled level of the thermal wavelength $\lambda_T = h \Big/ \left(2\pi m_n kT \right)^{1/2}$ and its scaled value $\lambda_T / \lambda_e = m_e c \Big/ \left(2\pi m_n kT \right)^{1/2}$ includes the atomistic (molecular) mass m_n together with the implied assumption of a uniform temperature field T. This mass-dependent combination $\left(m_n ; T \right)$ is absent in Eqs.(1–3) for the effective pairwise (unspecified here) 3-parameter FT-potential: $\phi^{FT}(r_{ij} \le r_f ; \varepsilon, \sigma_f, \lambda; n/6 -$ ratio of the repulsive *n* and the fixed $m = 6 -$ dispersion exponents) for $f -$ phase $\left(f = g \text{ or } l \right)$. The standard denotation of number density: $n = \rho / m_n -$ in the set for critical compressibility factor: $Z_c = P_c M \Big/ \left(\rho_c R T_c \right) = \; P_c \Big/ \left(n_c k T_c \right) = \; P_c^* \Big/ \left(n_c^* T_c^* \right)$; and the asymptotic Riedel's factor: $Ri^f \left(T \to T_c \right) = \left[d \ln \left(P_f / P_c \right) \Big/ d \ln \left(T / T_c \right) \right]_{\tau \to 1}$; $n_c^* = n_c \sigma^3$, $T_c^* = kT_c / \varepsilon$, $P_c^* = P_c \sigma^3 \Big/ \varepsilon$ has not to be confused with the only repulsive adjustable exponent *n* of FT-potential. The introduced by Eq. (4) FT-calibrated notion of *the atomistic (nucleon) mass density* for an effective spherical particle: $\rho_{nf} = 6m_n \Big/ \pi \sigma_f^3$ extends the Born-Oppenheimer's approximation on the

nanoscales of a single $f-$ phase [4, 5]. This approximation separates in the frame of isotopic concept the nearly mass-independent electronic structure of atoms determining most of their physico-chemical properties, from those involving nuclear motion. The local force-field of a particle related to its mass has the sense of perturbation correction to the mechanical acceleration $\varepsilon^{FT}\Big/\left(m_n\sigma^{FT}\right)$ in Eq. (4). This is the appropriate fluctuation component for any realistic nearly adiabatic conservative force-field: $f_{ij}=-\delta\phi_{ij}/\delta r_{ij}$ usable in the equilibrium MD-simulations. In addition to the basic unit of time adopted at the integration of Newton's equation: $\sigma\left(m_n/\varepsilon\right)^{1/2}$, it should determine, the longer time period taken for a particle to diffuse a distance equivalent to the approximate thermal $\lambda_T\left(m_n;T\right)-$ wavelength. The phenomenological FT-potential provides the useful theoretical tool for a comparative analysis of different elements and compounds. One needs only the critical point (CP) parameters [1-6] to map the mesoscopic criticality onto the set of its parameters by Eqs.(1-3) without any further fit and to probe the selected repulsive exponent *n*. The distinctive feature of FT-potential is also its finite reduced range of the direct interactions between particles controllable by the inverse PCS-factor of critical compressibility $\lambda^{FT}=Z_c^{-1}$ in Eq.(3).

The unique meaning of P_0-isobar modeling is corroborated by Eq.(23) in [1] for the asymptotic vicinity of the critical point. It appears to hold: $1-\tau_{sc}=Z_c\pi_0=P_0/n_ckT_c$ for any mesoscopic sizes of volume (i.e. volumes smaller than *its* $\left(P_c,T_c\right)-$*dependent correlation value*). This estimate of an asymptotic vicinity is fulfilled over the very high-temperature $(T_c-T_b)-$ range for metals. We note also that the problem of the very small scaling vicinity $\left(1-\tau_{sc}\right)$ in metallic vapors attribution either to the vdW-like class of mean-field *f*-criticality or to the Ising-like class of asymptotic lattice criticality can be unambiguously related to the non-mean-field type. The finite-range FT-potential of Eqs.(1-3) [2-6] is the most pronounced sign of a such possibility. The special FT-point of a maximum

associating attraction r_{ma} *determines not only the much deeper well-depth* ε^{FT} *but the large cohesive energy* $e_{coh}^{FT} r_{ma} \big/ \sigma_f^{FT} = e_{bind}^{FT}$ *of metals too*:

$$r_{ma} = \sigma_f^{FT} \left(n/6\right)^{2/(n-6)} < \sigma_f^{FT} \big/ Z_c \tag{5}$$

This n (repulsive exponent)-dependent correlation between the cohesive and binding energies is quite useful if $\Delta_v h \approx e_{coh}$ −value is unknown. The otained σ_f^{FT} – estimates are remarkably close for a variety of elements to the well-established *covalent diameters*. Thus, FT-model provides the mechanism of *interparticle* association in clusters of *f*-phase. Simultaneously, the last equality in Eq.(3) establishes an *exact scale-invariant connection* between the *well-depth* $\varepsilon^{FT} \big/ k$ from Eq.(1) and the *well-width* $\lambda^{FT} = 1/Z_c$.

In this context we remind that the indicative thermophysical PCS- factor Z_c is involved in all main FT-correlations based on the principle of global fluid asymmetry [1-6]. We represent their relevant forms below for the sake of completeness in terms of reduced PCS- variables $\left\{\tau = T/T_c, \pi = P/P_c, \omega = \rho/\rho_c\right\}$:

$$reference\ line\ (1.1): \quad \rho_l\left(P_0, T\right) = \frac{\rho_c}{Z_c}\left(1 - \frac{T}{T_0}\right), \tag{6}$$

$$g - phase\ branch\ (1.34): \quad Z_{gf}\left(\tau, \omega_{gf}\right) = \frac{Z_c}{\tau}\left(\frac{8}{3 - \omega_{gf}} - 3\omega_{gf}\right), \tag{7}$$

$$l - phase\ branch\ (1.35): \quad Z_{lf}\left(\tau, \omega_{lf}\right) = \frac{Z_c}{Z_c^0}\frac{1}{\left(1 - b_f \rho_{lf}\right)} - \frac{b_f \rho_{lf} T_0}{T}, \tag{8}$$

$$where: \quad b_f = \frac{4}{\rho_{nf}}; \quad Z_c^0 = \frac{3}{8}; \quad b_f \rho_c = \frac{Ri^f - 2}{2\left(Ri^f - 1\right)}; \tag{9}$$

$$metastable\ limit\ (1.30): \quad \omega_{ml}^2 - \frac{1}{Z_c}\left(2 - \frac{\tau}{18 Z_c}\right)\omega_{ml} + \frac{1}{Z_c^2}\left(1 - \frac{\tau}{9 Z_c}\right) = 0 \tag{10}$$

Both primary mean-field binodal/spinodal constructions never appear in FT-model due to the finite-range FT-potential meaning of Eqs.(1-3) at first and the

mentioned in [1] local failure of the Ehrenfest's classification *just in the close vicinity of a saturated l-phase* at second:

$$Ri_v = \frac{T}{P_v}\frac{dP_v}{dT} = \frac{M\left(C_{Pl} - C_l\right)}{Z_l RT\left(\alpha_{Pl} - \alpha_l\right)} > 0 \qquad (11)$$

Here $P_v(T)-$ the macroscopic single vapor-pressure curve (located for many compounds slightly downwards than the onset-boil curve $P_b(T)$ and significantly upwards than the onset-dew curve $P_d(T)$ of the *v*-interphase); $C_l = Tds_l/dT > 0$, $\alpha_l = dv_l/v_l dT > 0$, $C_{Pl} > 0$, $\alpha_{Pl} > 0$ and $Z_l = P_v v_l M/RT \to 0$ tends to zero just in the working "T – window" $T \le T_b\left(P_0, \rho_l\right)$ of IEX – measurements. Eq.(11) is typical for the structural second-order phase transition. However this immediate thermo-caloric generalization of the Clausius-Clapeyron's equation has been derived near the *l*-branch of the classical first-order $l \to v$ – transition by the elimination of $\beta_T -$ compressibility. In contrast to the global fluid asymmetry of FT-model, the role of this response function in the mean-field theory of a first-order transition is determinative (Section 1). Whereas the low-temperature trend $Z_l \to 0$ makes Eq.(11) to be hardly testable by the direct experiment in *v*-interphase, its resultant meaning remains invariable. As a result the *mhd* – instability can be explainable by the existence of *v*-interphase for the superheated metal at any arbitrary magnitude of its isothermal compressibility.

The similar FT-correlation was derived for the saturated *g*-phase only in the unified van der Waals' EOS frame. This result concerns the thermodynamic concept of existence in the $(T,s)-$ diagram [33] of the anomalous "dry" $(C_g = T\,ds_g/dT > 0)$, intermediate "isentropic" $(C_g = 0)$ and normal "wet" $(C_g < 0)$ types of gaseous LE-states:

$$\frac{C_{Pg} - C_g}{\left(s_g - s_l\right)^0} = 1 + \frac{Z_c^0 \tau}{1 - \tau} > 0 \qquad (12)$$

Here $\left(s_g - s_l\right)^0 = \pm 2kx/m_n$ is the $m_n -$ dependent *vdW – disorder parameter* in the exact FT-solution of the mean-field phase transition problem discussed in [1]. It was represented by Eqs.(31,33[1]) namely in terms of this reversible disorder parameter $\left(s_g - s_l\right)^0$. We have mentioned in [1] the special place of mercury in the set of liquid metals due to its critical: $Z_c^{\mathrm{Hg}} \approx Z_c^0 -$ value. It is expressed by the limiting $T_c^* -$ value in Eq.(1) for Hg: $T_c^{*\mathrm{Hg}} = kT_c/\varepsilon_0 = 1\Big/\left(1 - Z_c^0\right) = 1.6$ found at the additional $C_{Pg} = C_g > 0$ condition. This zero-numerator in Eq.(12) corresponds to the pseudo-ideal-gas trend: $\omega_{gf} \to 0$ in Eq.(34[1]). The proven so "dry" type of this anomalous heavy $(m_n^{\mathrm{Hg}} = 0.3336 \cdot 10^{-24}$ kg) thermometrical metal with its also zero enthalpy: $T_m\left(s_g - s_l\right)_m^0 = 0$ at the standard (s) melting point: $T_s = T_m = 298.2$ K[24] – opposes it to the normal "wet" water – the other very light standard thermometrical liquid $(m_n^{\mathrm{H_2O}} = 0.0299 \cdot 10^{-24}$ kg).

The thermodynamic inequalities of Eqs.(11,12) impose the stringent requirements of FT- consistency on the mutual changes of isobaric heat capacities C_{Pl}, C_{Pg} and isobaric coefficient of thermal expansion in a liquid α_{Pl}. At the low temperatures $T \le T_b$ both branches of sub-atmospheric pressure $P_f(T) \le P_0$ are determinable at the trend: $Z_l \to 0$ generating the secondary Zeno-line [27]. The following from the basic thermo-caloric Eq.(29[1]) at the marginal boil point equality: $(Z_{gb} = 1)$ defines the further change of vaporization enthalpy:

$$\frac{M\Delta_v h}{RZ_{gb}};\ T_c Ri^b \quad (a) \qquad Z_{gf}\left(T \le T_d = T_c Z_c \big/ Z_c^0\right) \ge 1 \quad (b) \qquad (13)$$

The conjugated equality (b) of Eq.(13) leads to the interesting pseudo-*soft-sphere* anomaly of saturated *gf*-phase at sub-atmospheric pressures. Its influence on the bulk properties (i.e the effective purely repulsive interaction of particles in the system of pair strongly attractive interactions) expressed by Eqs.(7,13b), may

indicate the induced conductivity for the real charged spheres. The physically plausible reason of such plasma-like transition is the synchronized sudden change of the effective *M*-value. It can provide the abrupt shifts of both gas-like factors: $Z_{gf} = \frac{P_f M}{RT\rho_{gf}}$ to the metastable liquid *ml*-values due to the co-operative clusterization of many constituent single atoms. The concomitant formation of liquid nano-droplets or their inverse destruction trend in *v*-interphase depends on the competing heat fluxes directed *from or to* the finite volume $(N,V)-$ system. The introduced by Eqs.(14-17[1]) polytropic derivatives: $\{\alpha \le T\alpha_P,\ \ \beta \le P\beta_T,\ \ Ri = \alpha/\beta \ge \alpha_P/\beta_T\}$ provide the reasonable mesoscopic alternative to the thermostatic integration alongside the isolines. The latters are often studied experimentally in the vicinity or inside the coexistence curve in spite of the apparent non-equilibrium nature of the mesoscopic phase transitions.

3. Critical points and congruent vapor-liquid diagrams for two soft metals: light Al and heavy Au

The concept of thermophysical unification induced by FT-model for the planed IEX-experiments and/or the imitating MD-simulations of liquid at atmospheric pressure P_0, picks out also the importance of two coupled normal points: T_b and T_d [1]. The specified so normal $T-$ width $T_d - T_b$ of *v*-interphase in different materials defines the condition for formation of an external metallic *v*-nano-structure on the surface of a wire-shaped sample. This effect leads unavoidably to growth of electrical resistivity and heat capacity in metals. The possible change of the surface conditions for radiation described by Plank's law becomes essential. In such context the comparison of two *soft* (the adopted characteristic of bulk *s*-phase) but simultaneously very different metals is challenging for the FT-universal predictive capability. Its theoretical "flexibility" could be additionally tested by the known trends to the oxidation, observable at the standard $(P_0,T_s)-$ conditions for light Al and heavy Au. This feature might be

conjecturally related to the above distinction, provoked also by the large difference of porosities $\varepsilon_l = 1 - b\rho_l$ from Eq.(8) introduced by Eq.(31b[1]) for *l*-phase.

The exact FT-correlation *f* = (*b* or *d*) connects the critical and both normal points:

$$M\Delta_f h\left(T_f\right)\Big/R = T_c T_f \ln\left(P_c/P_0\right)\Big/\left(T_c - T_f\right) \tag{14}$$

It follows at P_0 from the thermo-caloric congruence of Eq.(29[1]) with the testable by the direct experiment combination of Z_f −factors: $\left\{Z_{gf}\left(T_f\right)=1,\ Z_{lf}\left(T_f\right)=0\right\}$. Fortunately, the comprehensive review and analysis of discrepancies reported by Zhang et al [32] for the $\Delta h_v\left(T_b\right)$−correlations published in different thermophysical handbooks is available. The useful PCS- correlations of melting point $T_m\left(\varepsilon/k\right)$ and critical point $T_c\left(\gamma_l\right)$ as a function of surface tension was discussed in [30,31] by Blairs and Abbasi. It follows from those that the selection of 4 indicative FT- parameters [1] $\{\rho_0,\ T_0;\ T_b;\ \left(M/R\right)\Delta_b h\}$ for metals is the *absolutely non-trivial task*. The rare caloric measurements and/or concomitant EOS' – estimates show that the recommended T_b- and $\Delta_v h-$ values often fall into two groups of poorly consistent smaller and larger enthalpies of vaporization: $\Delta_v h_1\left(T_{b1}\right) < \Delta_v h_2\left(T_{b2}\right)$ where $T_{b1} > T_{b2}$ [32]. The T_m- and T_c- estimates are appropriate for metals, at best, for comparison. The independent FT- prediction of critical point by Eqs.(18,22[1]) on the base of input parameters provides the desirable well-tested unification:

$$\ln\frac{R\rho_0 T_0^2}{81MP_0} - \frac{M\Delta_b h}{RT_b} = \ln T_c - \frac{M\Delta_b h}{RT_c}, \tag{15}$$

$$\rho_c = \rho_0 T_0\Big/\left(9T_c\right)\quad (a) \qquad P_c = \rho_c RT_0\Big/\left(9M\right)\quad (b) \tag{16}$$

3.1 Aluminum $(M = 27\ \mathrm{g\cdot mol^{-1}})$

Al is an example of widely-studied by static and dynamic experiments at low and moderate temperatures metal [8,13,15]. Hence the discrepancies in the

reported estimates of critical parameters for it are still unacceptably large. They are represented in Table 1 together with the recommended FT- estimates of this work.

Table 1 Comparison of FT-critical point for Al with its mean-field estimates and the Boyle's type input parameters of other authors (the omitted here and obviously overestimated T_c- values $(7400\,\mathrm{K} \le T_c \le 8900\,\mathrm{K})$ and respective ρ_c, P_c- values can be found elsewhere [22,29])

T_c, K	ρ_c, kg·m^{-3}	P_c, bar *)	Z_c **)	ρ_B, kg·m^{-3}	T_B, K	$M\Delta_v h/R$, K	Ref.
4500	550						[13]
5726	424	1820	0.24(3)				[24]
6890	470	1806	0.18(1)	2620	14100		[29]*)
6989	365	1071	0.137	4600	12900	34188	[29]*)
6989	360			1250	12900	35340	[29]*)
5698	566	3930	0.396				[22]
6063	556	3730	0.359				[22]
6586	563			2590	11130		[27]*)
6518	424.5	1369	0.1607	2642	9426	34159	FT

*) – the significant uncertainty of the primary [26] and secondary [27] Zeno-line methods at the estimation of $(\rho_B, T_B)-$ parameters is compared here with our $(\rho_0, T_0)-$ input parameters selected for Eq.(1.1)(see text and Table 2 below).
**) – the values in brackets are added to consist the reported parameters.

To select the necessary and enough 4 input parameters of the P_0- isobar $\{T_0,\ \rho_0;\ \Delta_v h(T_b),\ T_b\}$ represented in Table 2 for the trial T_c- estimation by Eq.(15), the following sequence of steps is necessary. We have considered, at first, the important practical option: the reasonable experimental compatibility of the static and dynamic measurements of density. The formers are performed usually near the melting point $T_m \le T \le 1500$ [13,15], while the older high-pressure IEX-data of Gathers [8] – in the much wider temperature ranges. The recent low-pressure dynamical ohmic pulse-heating data of Leitner et all [13] are reported up to $T \approx 1700\,\mathrm{K}$. The vdW / soft-sphere unified EOS developed in [23,24] was still based on the static LE-data. Young has shown that it is able to extend inessentially the relatively short T – range only up to $T = 1800\,\mathrm{K}$ for Al. The reliable estimation

of cohesive energy: $e_{coh} \approx \Delta_v h(T_b)$ is the crucial factor to reestablish CVL-diagram.

Table 2 The influence of static and dynamic experimental $(\rho_0, T_0)-$variations of input points on the location of FT-critical point predicted for Al at the common selected (see text) $\left\{T_b^{\mathrm{Al}} = 2743\ \mathrm{K};\ \Delta_b h^{\mathrm{Al}} = 284\ \mathrm{kJ \cdot mol^{-1}}\right\}$ values from [32].

Range T, K	ρ_0, $\mathrm{kg \cdot m^{-3}}$	T_0, K	ρ_0/T_0, $\mathrm{kg \cdot m^{-3} \cdot K^{-1}}$	T_c, K	ρ_c, $\mathrm{kg \cdot m^{-3}}$	P_c, bar	Authors, Ref.
$[T_m;1190]$	2668	8577	0.311	6340	401.0	1177	Assael et al [15]
$[T_m;1495]$	2553	9562	0.267	6510	416.7	1363	Leitner et al [13]
$[T_m;1680]$	2670	8930	0.299	6420	412.7	1261	Leitner et al [13]
$[T_m;4000]$	2698**)			5726***)	424***)	1820***)	Gathers [8]*)
$[T_m;3100]$ **)	2642	9426	0.280	6518	424.5	1369	T_{mhd}^{Al} – FT

*) – both quadratic functions $h_l(T)$ and $v_l(h_l)/2698$ used in [8] to fit IEX – data for $P = 0.3$ GPa need the *FT – calibration* (Section 2,4) to eliminate the supposed inconsistence induced by the interpretation of IEX-equilibrium temperature $T-$ value.

**) – $T_{mhd}^{\mathrm{Al}} \approx 3100$ K is here estimated by Figs.1,2 and corresponds to the condition $1/Z \geq \lambda$.

***) – Young [24] obtained these *mean-field* critical parameters by usage of the well-interconnected low-pressure dilatometric measurements reported by Gol'tsova and the highly non-equilibrium Wilson's data [8].

Unfortunately, the detailed compilation of the necessary macroscopic input parameters $\left\{T_b; \Delta_v h(T_b)\right\}$ reported by Zhang et al [32], demonstrates their essential inconsistency in the different databases. To avoid any exclusions based on judgement or adjustment, we have tested for Al both inherently inconsistent pairs $\left\{T_b = 2743\ \mathrm{K};\ \Delta_v h = 284\ \mathrm{kJ \cdot mol^{-1}}\right\}$ and $\left\{T_b = 2793\ \mathrm{K};\ \Delta_v h = 294\ \mathrm{kJ \cdot mol^{-1}}\right\}$ from [32]. Such test should exclude an inconsistency since the larger heat of vaporization along the single macroscopic $T-$dependence should always correspond to the lower temperature. The physically natural FT-attempt to explain the presence of above inconsistent experimental pairs is simple. We proposed the

dew-point identification of the larger normal value: $T_d = 2793\,\mathrm{K}$. It belongs to $P_d(T)-$bound of *v*-interphase which is located for Al slightly above (: $50\,\mathrm{K}$) $P_b(T)-$bound. This assumption was supported then by the concept of mesoscopic irreversibility [1] at $P_0 = const$: $\left|\Delta_d h(T_d)\right| = 294\,\mathrm{kJ\cdot mol^{-1}} > \Delta_b h(T_b) = 284\,\mathrm{kJ\cdot mol^{-1}}$. We have used this conjecture in Eq.(26[1]) for the exact and consistent prediction of $T_c^{\mathrm{Al}} = 6518\,\mathrm{K}$ and $T_0^{\mathrm{Al}} = 9426\,\mathrm{K}$ (Tables 1,2). This result was obtained namely at the selected cohesive energy and the fixed now normal boiling point $\left\{T_b = 2743\,\mathrm{K};\ \Delta_v h = 284\,\mathrm{kJ\cdot mol^{-1}}\right\}$ for aluminum.

Some comments to the described estimates of $(\rho_0, T_0)-$parameters for Al are very informative because the posed task of experimental compatibility has been convincingly solved. Indeed, the deviation between critical parameters based on the electromagnetic levitation data obtained by Leitner et al [13] and those inferred from their pulse-heating experiments is comparable with the recommended FT-estimates in Tables 1,2 within the experimental uncertainties of slopes $\rho_0/T_0(\pm 10\%)$. At the same time, neither the variety of modified mean-field estimates including ones in [13] (Table 1) and [24] (Table 2) nor the rather sophisticated PCS- correlations [21,22,30,31] for the cohesive energy are able to solve the task of choice. The claimed PCS-prediction of an a priori unknown set of critical parameters *on the base of density measurements exclusively* in a low-temperature liquid is not possible or hardly realizable. One needs additionally the two-phase enthalpy. At the given $\{T_b, \Delta_b h\}-$ values we estimate the percentage uncertainties of critical FT-point for $T_c(\pm 3\%)$, $\rho_c(\pm 6\%)$, $P_c(\pm 15\%)$.

Table 3 (a) – FT-factors for aluminum named by us for Riedel (Ri), Guldberg (Gu), Trouton (Tr), Guggenheim (B_l) are predicted by Eqs.(1.26-1.30) and testable by Eqs.(5-9). (b) – to facilitate the test all key points (Section 2) are calculated for comparison with the available experiment.

f – branch	Gu^f	Ri^f	Tr^f	B_l^f	(a)
$f = b$ (boil)	0.42085	5.2407	12.453	1.51910	(a)
$f = d$ (dew)	0.42853	5.4081	12.620	1.51457	(a)
$M = 27\ \mathrm{g\cdot mol^{-1}};\ \rho_0^{\mathrm{Al}} = \rho_{ml}(T \to 0) = 2642\ \mathrm{kg\cdot m^{-3}};\ T_0 = T_{ml}(\rho \to 0) = 9426\ \mathrm{K}$					
T, K / ρ, kg·m^{-3}	$T_s = 298$	$T_m = 933.2$	$T_b = 2743$	$T_d = 2793$	(b)
ρ_{lb}	2310	2202	1873	1863	(b)
ρ_{ld}	2304	2197	1869	1859	(b)
ρ_{l0}	2558 *)	2380 *)	1873	1859	(b)
ρ_{ml}	2288	1985	1424	1411	(b)

*) – Young [24] used these input densities of solid and melt liquid to solve the system of equalities for vacuum assumed at the melting point T_m: $P(\rho_{lm}, T_m) = 0;\ h(\rho_{ml}, T_m) = e_m$ for the vdW / soft-sphere mean-field EOS (see Table 2 for its prediction of critical point).

This predictions are rather sensitive to the variation of the vaporization enthalpy: $\Delta_b h \approx e_{coh}$ with its very large uncertainties [32]. For example, the choice by Young [24] of the increased $(:\ 14\%)$ input cohesive energy: $e_{coh}^{\mathrm{Al}} = 12200\ \mathrm{kJ\cdot kg^{-1}}$ instead of that in Table 2: $e_{coh}^{\mathrm{Al}} \approx \Delta_v h^{\mathrm{Al}} = 10519\ \mathrm{kJ\cdot kg^{-1}}$ has significantly shifted the predicted critical mean-field density just to its non-mean-field FT- value. The shown failure of a rectilinear diameter rule in Fig.1 is typical feature for all other 12 fluid metals studied by CVL- diagram [1-3]. Thus the proposed thermophysical unification is realizable by the FT-prediction of CVL-diagram in Table 3 without the further fit and any empirical coefficients. The predictive capability is corroborated by the several comparisons illustrated in Fig.1. The parameters $\{T_c, \rho_c, P_c; Z_c\}$ of FT-critical point in Tables 1,2 are located systematiacally lower than those from the many unified EOS-based sets of parameters in the different variants of Zeno-line-method [26,29]. The exploratory usage of the rectilinear diameter is typical for it. Another noticeable comparison concerns the irresolvable nature of a mean-field critical point prediction. The underlying discrepancy between the thermal and caloric variants of such extrapolative procedure leads either to the significantly underestimated by PCS or to the very overestimated by the unified EOS $T_c -$ values for a metallic melt. The application of the primary Zeno-line-concept [26] in a combination with the simulated isobaric high-pressure

$P \geq 0.1\,\text{GPa}$ data for Al was reported in one of the previous works of authors [29]. The results obtained on the base of standard embedded atom *N*-body potential [18] lead to the thermodynamically questionable tendency. This is an artificial *non-congruent* (*not everywhere convex*) $\rho_l(T)-$ *branch* of $l \to v$ *– diagram* for so called "bad" (refractory and rigid) metals. Authors [29] used the specially changed tabular $M\Delta_v h/R-$ value (Table 1) in the Zeno-line Eqs.(24,25[1]) seemingly to avoid of this undesirable trend for "good" Al. FT-model predicts the coupled values $T_c = 6518\,\text{K}$ and $Ri^b = 5.2407$ by Eq.(13a) in the complete coherence with the recommended experimental value $M\Delta_v h/R - 34159\,\text{K}$ [32] in Table 1. This

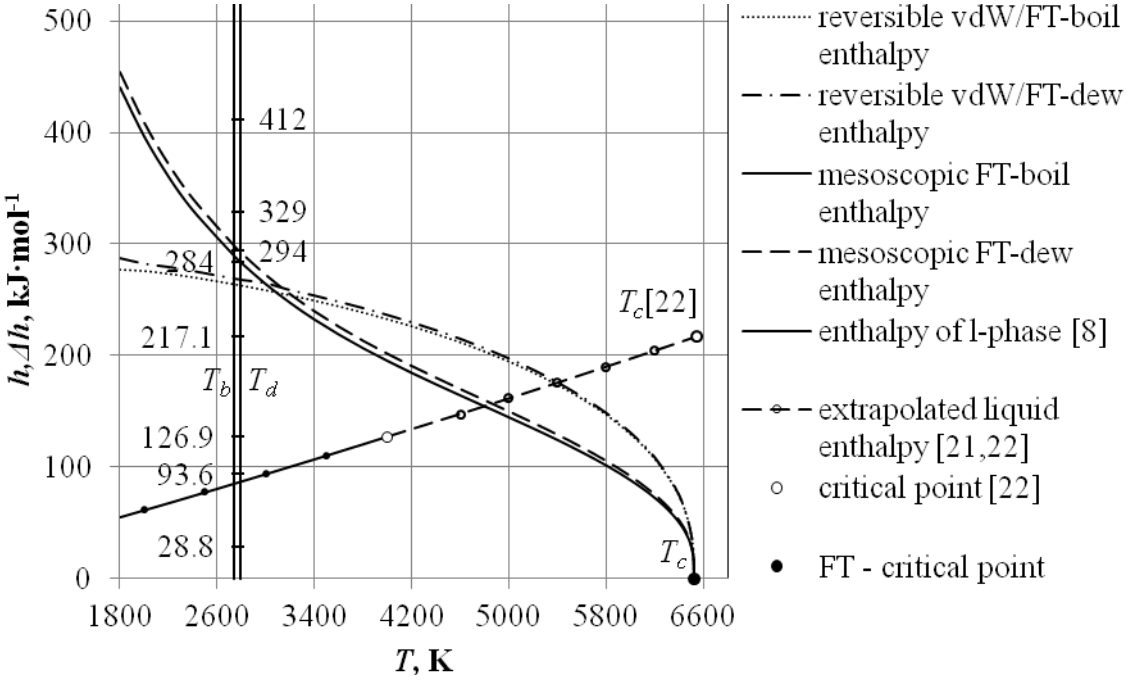

Fig.2 Thermal hysteresis of the dynamic non-equilibrium vaporization– condensation process. Its local mesoscopic irreversible transformation is predicted for nano-scales of the gaseous and liquid Al. The onset of transition loop occurs in both metals Ta [1] and Al at $T \geq T_d$ as it is shown by two thin vertical lines for Al at $T \geq 3 \cdot 10^3$ K (see also Fig.1). We delineated by the set of bold horizontal dashes the following levels of cohesive energy estimated by its different models (from top to bottom): 1) T – independent e_{bind}^{FT} (Eq.4); 2) e_{coh} [27]; 3,4) $\Delta_f h$ [32]; 5) $e_{coh}^0(T_m)$ [21]; 6) $h_{mhd}(T = 4000\,\text{K})$ [8]; 7) $h_{mhd}(T \approx 3000\,\text{K})$ 8) $h_m(T_m)$ [8,13]. The long-range extrapolation of IEX supercritical $h(T)-$ data [8] used in [21,22] to estimate the realistic T_c (Table 1) is shown by the dashed-dotted line

option becomes possible due to the thermo-caloric congruence of CVL-diagram.

The phenomenon of thermal hysteresis represented by the caloric projection of Fig.2 for Al confirms its "wet" type of $T,s-$diagram similar to that for molecular light fluids H_2O [4] and CH_4 [5]. The sequence of depicted curves in the wide high-temperature segment T_c-T_d of the one-phase $(h,T)-$ and two-phase $(\Delta h,T)-$projections is different from that shown earlier in Fig.(5[1]) for the supposedly "dry" refractory Ta. Both sets of curves were obtained: 1) by the substitution of predicted CXC-densities (Fig.1) in Eqs.(31-33[1]) to estimate the disorder parameter $\left(s_g-s_l\right)^0 m_n \big/ 2k$ for the reversible FT / vdW- solution; 2) by their alternative usage in the general FT-thermo-caloric Eq.(29[1]). The comparison of both ones implies an irreversibility of the *heterogeneous nucleation* in *v*-interphase. The change of an effect sign at the intersection of all branches (i.e. the supposed breakpoint of instability $T_{mhd}\geq 3000$) is interesting. Our result supports in particular the concept of its occurrence *near and slightly above the coexistence curve* (*i.e. above the binodal temperature* of the mean-field approach) [17] *but not at the spinodal temperature* as its variant [16]. The effect is detectable *for supercritical isobars* as well. The *classical cubic spinodal* considered with the actual FT-critical point (Fig.1): $\omega_{sp}^3-6\omega_{sp}^2+9\omega_{sp}-4\tau=0$ is also shown in $(\omega,\tau)-$plane. The goal is to compare with the exactly predicted by Eq.(10) *non-mean-field quadratic FT-limit* of a mesoscopic metastable *ml*-phase. We emphasize now that the variety of extensive efforts to develop the *spinodal – decay mechanism* of the exploding wires by focusing exclusively on the liquid phase properties needs the serious revision. It may be either misdirected experimentally at the estimation of critical point or be too restrictive theoretically by the usage of a homogeneous nucleation constraint. One of such attempts is illustrated in Fig.2 by the long-range extrapolation of the *supercritical* Gathers' low-temperature fit of IEX-data for Al [8]. This construction was used by Morel et al [22] to estimate T_c- value *on the ad hoc basis* of its further elongation in the critical region.

We have combined in Fig.3 the previous FT-results for the refractory Ta with the results for Al (Fig.4[1]). For Ta two evident trends to the sharp separation between the melting T_m and vitrification T_g temperatures have been established.

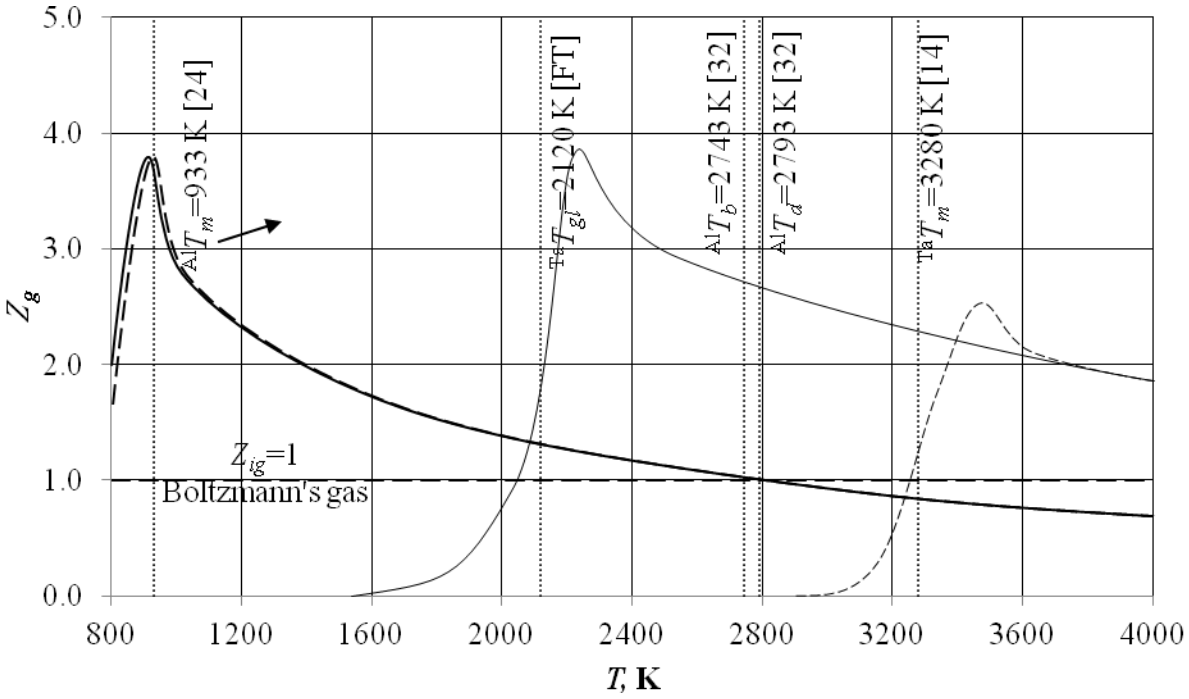

Fig. 3 The comparison of two anomalous "low-temperature" ranges of the pseudo-soft-sphere $\left(Z_{gf} > 1\right)$ – values of gaseous compressibility factor predicted at sub-atmospheric pressures for Al in this work and for Ta in [1]. Both regions are located between the equilibrium melting points: $T_m^{\mathrm{Al}} = 933.2\ \mathrm{K}$, $T_m^{\mathrm{Ta}} = 3280\ \mathrm{K}$ and boiling points: $T_b^{\mathrm{Al}} = 2743\ \mathrm{K}$ (both normal points $T_b^{\mathrm{Ta}} = 5731\ \mathrm{K}$ and $T_d^{\mathrm{Ta}} = 7482\ \mathrm{K}$ - lie outside the region shown). Two predicted around the melting point for Al characteristic limits of under-cooling for gas/boil-branch and superheating for gas/dew-branch correspond reasonably to the reported nucleation limits [18]. Inset: FT- predicted inessential split in mesoscopic phase-transition for Al

For Al the FT-prediction demonstrates the only former trend to melting observable experimentally [15]. Thus, the peculiarity of pseudo-soft-sphere behavior in a gaseous phase below T_d (see Eqs.7,13b) and its predictive capability for the estimation of T_m and T_g are completely consistent with the experimental observations.

3.2 Gold $(M = 197\ \mathrm{g \cdot mol^{-1}})$

The further verification of the natural scepticism about the existence and role of a mean-field spinodal is especially worthwhile for metals. We compare the dynamic IEX- prediction of unknown critical point with FT-estimates concerning the soft but heavy Au. The direct dynamic experimental determination of critical point based on the concept of spinodal for Au was reported by Boboridis et al [12]. It facilitates our consideration and has been earlier supplemented by the one-phase IEX-results for liquid gold of Kaschnitz et al [11]. The experimental points for the usual set of density, enthalpy and electrical resistivity $\{h, \rho, \rho_e\}$ were approximated by these authors by the simple mutual linear correlations. The Plank's law calculation of temperature was performed at different high pressures to extend the range of *l*-phase by suppressing boiling up to the spinodal points. Authors [11,12] considered the IEX-equilibrium thermostatic interpretation of obtained critical data represented for comparison in Table 4.

Table 4 Comparison of two variants for FT-critical point (see text) predicted for gold with its mean-field estimate [12] on the basis of the same $(\rho_0, T_0)-$ parameters from [11]. Comparison with the other mean-field estimates taken here from [12] is also represented.

T_c, K	ρ_c, $\mathrm{kg \cdot m^{-3}}$	P_c, bar	Z_c	P_c/ρ_c	ρ_0, $\mathrm{kg \cdot m^{-3}}$	T_0, K	Investigator (first author)
7400±1100	7692±1900	5300±200	0.2206	0.689	19033	13187	Boboridis, 1999 [12]
5557	549.5	376	0.2918	0.684			Gates, 1960
8100	4348	4620	0.3108	1.063			Morris, 1964
8267	5000	6265	0.3591	1.253			Young, 1971
8077*)	3453	2135	0.1814	0.618	19033	13187	$T_{b_1}, \Delta_b h$ [32]
8160	3418	2113	0.1795	0.618	19033	13187	$T_{b_2}, \Delta_d h$ [32]

*) – we have selected for the further prediction of CVL-diagram in Table 5 the upper (similar to the choice for Al in Table 2) variant $\{T_b = 3123\ \mathrm{K};\ \Delta_b h = 324\ \mathrm{kJ \cdot mol^{-1}}\}$ corresponding to the FT concept of irreversibility [1] and $\rho_0/T_0 = 1.4433\ \mathrm{kg \cdot m^{-3} \cdot K^{-1}}$ [11].

The integral enthalpy during the fixed $\Delta t-$interval of time is the most accurate quantity of IEX-measurements. It was supposed earlier that its non-

equilibrium Joule-Lentz nature requires the correction for irreversibility [1]. The proposed below way to take it into account, was termed *FT-calibration*. It implies the comparison of measured enthalpy without (non-equilibrium) and with (equilibrium) correction imposed by the thermal polytropic (non-isobaric) expansion $\alpha = Tdv/vdt$. Its scaling $T-$dependence $\alpha = T/(T_0 - T)$ is important because of the postulated irrelevance of ρ_0-value. The proposed FT-calibration is realizable (Section 4) just by a *simultaneous multitude refinement* of all $t-$dependent ingridients in Eq.(36[1]) including the ratio of electrical resistivity $\rho_e(t)$ to density $\rho(t)$. We have supposed in Section 2 that the absence of synchronization between the essentially non-linear $T(t)-$dependence (inferred from the equilibrium thermal radiance condition) and the non-stationary Ohm's law may lead to the inconsistency. The irreversible current $I(t)-$ and voltage drop $\Delta U(t)-$data should be transformed to avoid the reported so IEX-discrepancies. The concept of *v*-interphase supposes the appearance of the electrically much worse conducting heterogeneous structure on the liquid surface of a wire-shaped sample after T_m-point. Probably, it is the distorting factor even for the correctly estimated but integral effect of a rate $\Delta T/\Delta t$ [1].

Table 5 The standard set of recommended FT-factors $\{Gu^f, Ri^f, Tr^f, B_l^f\}$ for gold (a) and the predicted FT-data for comparison with key points (b)

$f-$branch	Gu^f	Ri^f	Tr^f	B_l^f	(a)
$f = b$ (boil)	0.38665	4.8245	12.478	1.38657	(a)
$f = d$ (dew)	0.44837	7.1704	14.823	1.35779	(a)
$M = 197\ \mathrm{g\cdot mol^{-1}};\ \rho_0^{\mathrm{Au}} = \rho_{ml}(T\to 0) = 19033\ \mathrm{kg\cdot m^{-3}};\ T_0^{\mathrm{Au}} = T_{ml}(\rho\to 0) = 13187\ \mathrm{K}$					
T, K / ρ, $\mathrm{kg\cdot m^{-3}}$	$T_s = 298$	$T_m = 1337$	$T_b = 3123$	$T_d = 3907$	(b)
ρ_{lb}	17287	16463	14526	13607	(b)
ρ_{ld}	17229	16193	14296	13394	(b)
$\rho_{l0}(P_0 = 0.1\ \mathrm{MPa})$	18603	17103	14526	13394	(b)
ρ_{ml}	16902	14240	11262	10165	(b)
$\rho(P = 0.2\ \mathrm{GPa})$	19300	17100	14500	13400	(b)

We have used to elucidate the situation just the represented in [11] linear function in the form of Eq.(1[1]). It provides the fixation of following input FT-parameters for Au: $\rho_0 = 19033\,\mathrm{kg\cdot m^{-3}}$; $T_0 = 13187\,\mathrm{K}$. The respective slope common for all isobars ranging from $P_0 = 1\,\mathrm{bar}$ to $P = 0.2\,\mathrm{GPa}$ was so fixed too: $\rho_0/T_0 = 1.4433\,\mathrm{kg\cdot m^{-3}\cdot K^{-1}}$. In this case our aim is the estimation of a *cumulative effect of input uncertainties* (term from subsection 1.2.3 in [1]) induced *at the given* large slope. The issue is a possible discrepancy in the reported $\{T_b;\Delta_v h(T_b)\}-$ parameters for Au. Zhang et al [32] related gold to the best category of elements for which these parameters are consistent: $\{T_{b_1} = 3123\,\mathrm{K};\ \Delta_{b_1} h = 324\,\mathrm{kJ\cdot mol^{-1}}\} \le \{T_{b_2} = 3243\,\mathrm{K};\ \Delta_{b_2} h = 342\,\mathrm{kJ\cdot mol^{-1}}\}$ within the reasonable experimental uncertainties. However, the situation resembles the thermostatic inconsistency for a single $\Delta_v h(T)-$ curve described in the previous Subsection 3.1 for Al. Hence we will try out once more to identify: $T_{b_2} = T_d$ with the normal dew point of *v*-interphase. This assumption *discovers immediately the drastic distinction between two soft metals Al and Au*. It was hypothesized in Section 2 as the difference between "wet" and "dry" types of $(T, s_f)-$diagrams for the light and heavy metals, respectively. The predicted by Eq.(13) $T-$width for the hypothetically "dry" gold $(T_d^{\mathrm{Au}} - T_b^{\mathrm{Au}}) = 784\,\mathrm{K}$ is much wider than its assumed above conjectural estimate $(T_d - T_b) = 120\,\mathrm{K}$ from [32]. Moreover, the predicted by FT-model dew point $T_d = 3907\,\mathrm{K}$ in the both completely compatible variants of critical point (Table 4) is again very close to the limiting point of instability: $T_{mhd} = 3820\,\mathrm{K}$ [11]. This value was revealed at the high but *still subcritical ambient pressure* $P = 0.2\,\mathrm{GPa}$. To stress its observable FT-irrelevance in liquid at the IEX-estimation of densities, two isobars $P_0 = 0.1\,\mathrm{MPa}$ and $P = 0.2\,\mathrm{GPa}$ are represented in Table 5. The well-established by CVL-diagram long-range extrapolation of

$\rho_{lf}(T)-$dependences demonstrates the similar densities of a saturated mesoscopic condensed matter at the very different ambient pressures. The macroscopic measurements along P_0-isobar are definitely enough for the reliable and consistent FT-predictions of critical point (Table 4). The suppressing boiling by the higher ambient pressures is indeed the only role of an external medium to avoid the thermal explosion [11]. It is most likely that the soft gold with its very high density and sharp slope ρ_0/T_0 belongs namely to the same "dry" fluids as the other heavy but refractory metal Ta.

The "Procrustean bed" of the mean-field spinodal/binodal formalism and a plausible, useful for the sketch of $l\to v$-diagram thermostatic consideration is still questionable for nanoscales. The unified EOS-concept leads to the variety of unsuccessful attempts "to bring" the actually observable phenomenon of *mhd*-instability to the region of spinodal decay. Besides, such an attempt is the obvious obstacle for the realistic estimation of critical pressure P_c and critical density ρ_c. The confirmation of this restriction is represented in Table 1 for Al and in Table 4 for Au. We have confirmed the relevance of the consistent $(T_d-T_b)-$ width for *v*-interphase and the role of T_0- point in this problem. Eq.(26[1]) determines its proportionality with the hypothesized here T_d- origin of any dynamic instability.

Table 6 Comparison of FT-potential parameters ε^{FT}/k, $\sigma_f^{FT}=(\sigma_g+\sigma_l)/2$ and the binding energy $e_{bind}\left[\mathrm{kJ\cdot kg^{-1}}\right]$ from Eq.(4) with the Chapman's PCS-correlation ε/k *)$=5.2T_m$ [30], tabular covalent diameter σ_{cov} and the cohesive energy: $e_{coh}\approx\Delta_v h\left[\mathrm{kJ\cdot kg^{-1}}\right]$ [24].

Fluid	M, $\mathrm{g\cdot mol^{-1}}$	ε^{FT}/k, K	ε^{Ch}/k, K	σ_f^{FT}, nm	σ_{cov}, nm	e_{bind}^{FT}	e_{coh} [24]	ρ_{nf}/ρ_c
Al	27	5471	4853	0.2686	0.248	15423	12200	10.4
Ta	181	9609	17056	0.2529	0.268	4242	4319	9.11
Au	197	6612	6952	0.2611	0.268	2597	1645	10.2

*) – the only preferable here Chapman's correlation for ε/k is based on the experimental viscosity and self-diffusion, both dependent explicitly on the particle (nucleon) mass

$m_n = M/N_A$ as well as the binding FT-energy is in Eq.(4).The ratio $\left(e_{bind}/e_{coh}\right)^{FT}$ from Eqs.(4,5) is only *n* (repulsive exponent) – dependent. Similarly to the other parameters of FT-potential from Eqs.(1-3) it is m_n – independent.

The interesting conclusions follow from the CVL-data of Tables 1-5 for Al and Au and Tables 1-2[1] for Ta compared with the empirical PCS-correlations reported by Blairs and Abbasi [30,31]. In Table 6 we represented the recommended parameters of FT-potential from Eqs.(1-5) and the respective data for three metallic melts including those estimated by the sharply different PCS-correlations: $\varepsilon/k = 5.2\,T_m$ (Chapman, 1966), $\varepsilon/k = 1.32\,T_m$ (Collings, 1974), $\varepsilon/k = 0.246\,T_m$ (Abbasi and Blairs, 2006). The only older one rejected then by all other authors [30] predicts the consistent magnitudes of well-depth ε/k compatible with the FT-potential estimate Eq.(1). For refractory Ta even this Chapman's PCS-strategy of prediction [30] based on the T_m – value fails. T_m was not included by us in the set of input parameters but is reliably predicted here.

In [31] the PCS-correlation based in this case on the T_b – value was proposed in the empirical form: $1.0788 \ln T_b = \ln\left(T_c/1.2574\right)$ where the old correlation recommended by Hirschfelder et al for all Lennard Jones' fluids: $\varepsilon_0/k = T_c/1.2574$ had been accepted. The selected by us experimental T_b – values from [32] give T_c – estimates for Al (Table 2): $T_c^{\mathrm{Al}} = 6436\,\mathrm{K}\,(-1.3\%)$, for Ta (Table 1.1): $T_c^{\mathrm{Ta}} = 14251\,\mathrm{K}\,(14.8\%)$ and for Au (Table 4): $T_c^{\mathrm{Au}} = 7403\,\mathrm{K}\,(-8.3\%)$. It is very likely that the IEX-experimental mean-field estimate for gold $T_c^{\mathrm{Au}} = 7400\,\mathrm{K}$ from [12] was used in [31] to determine the "universal" PCS-coefficient 1.0788 for all other metals. However, it follows from Table 4 that the comparable T_c – values, obtained by the direct predictive methods, can lead to the quite different P_c – and ρ_c – estimates. One cannot dwell in such case on the issue of the actual criticality, although the additional controllable factors of the predictive consistency: $\{Z_c;\ P_c/\rho_c = Z_c RT_c/M\ ;\ Z_c kT_c/m_n\}$ could form the useful criterion for the ultimate

choice. The remarkable correlation of the binding energy e_{bind}^{FT} with the conventional determination through the measurable $\Delta_v h-$value of cohesive energy e_{coh} is noticeable. Its FT-model counterpart e_{coh}^{FT} in Table 6 predicts the meaningful consistency with the tabular covalent $\sigma_f^{FT}-$diameter.

4. FT-calibration of IEX-data attributed to the fast polytropic processes of measurements in Ta and Al

We assume [1] that LE-conditions are not definably fulfilled during the concurrent dynamical trends to a cluster generation of *v*-interphase and a metastable liquid structure formation. This assumption should be distinct from the conventional LE-supposition at the IEX-treatment by the quadratic or other $T-$ functions [7-9]. The term of *irreversible IIEX-process* will be applied below to the polytropic by its inherent nature change of the measurable variables $\{h,\rho,\rho_e;T\}$ for this purpose. Their convertation into the thermodynamically consistent complex of thermo-physical variables should be mutually coherent. FT-calibration is not concerned about the necessity of the exclusively electromagnetic interpretation of evaporation in metals arising due to the pulsatory high-density electrical currents: : j_q^2 from Eq.(36[1]). In contrast the driven FT-force of *mhd* – instability has to be formally considered within the frame of polytropic process as a cross-effects' result of thermo-diffusion (Soret effect), thermo-electrical diffusion (Peltier effect) and electro-diffusion (Nernst effect). This observation applied to the single IIEX- shot leads to the invariant polytropic heat capacity $C^{FT}(T)=\rho^{-1}dP/dT$ of any LE-change by the well-motivated FT- assumption. The latter quantity unifies [1] the real inhomogeneous characteristics of a fast thermal expansion. It should reflect the postulated here inertia of the above diffusion cross-effects occurred inside of a metallic wire-shaped sample: $\alpha^{FT}\le T\alpha_P=T/(T_0-T)$. This formal $T-$dependent consequence of the FT-

model's P_0-isobar expands Eqs.(1-2[1]) on the other low-temperature ambient isobars including all sub-critical and super-critical ones. We consider this presumable invariance of IEX-data as the crucial controllable factor for FT-calibration. Its main aim is the subtraction of LE-contributions $\left\{h^{FT},\ C^{FT},\ P^{FT},\ \rho_e^{FT};\ \alpha^{FT}\right\}$ from the combined by Eq.(36[1]) IIEX- measured irreversible $t-$dependent characteristics $\left\{\delta h_{JL},\ C_{JL},\ j_q^2,\ \rho_e,\ \rho\right\}$.

4.1 FT-calibration of metastable [1] subcritical $\left(P=0.3\,\text{GPa}\right)$ IEX-data for tantalum [7].

We have selected the rather challenging case of heavy Ta to demonstrate the proposed FT-calibration steps (Section 2). This metal was measured several times by different authors with the unsuccessful efforts to decrease the resultant too high specific heat capacity $C_{JL}\left(T\right)$. The reported Gathers' IEX-data [7] were identified by CVL-diagram as the completely metastable ones (Fig.1[1]). We will compare below the percentage deviations of FT-calibraation $\delta_a\%=\left(a^{FT}/a[7]-1\right)\cdot 100\%$ for quantities of interest α^{FT} and T^{FT} in Table 7. Our purpose here is to reach the final estimate of density $\delta_\rho\%$ by comparison with the low-pressure stable (interpolated) IEX-data reported by Leitner et al [14] and used in [1] as the input $\left(\rho_0^{FT},T_0^{FT}\right)-$parameters.

Table 7 FT-calibrated *polytropic thermal expansion*: $\alpha^{FT}=\ \alpha[7]\rho[7]/\rho_0^{FT}$ $(\rho_s[7]=16600\,\text{kg}\cdot\text{m}^{-3};\ \ \rho_0^{FT}[1]=17250\,\text{kg}\cdot\text{m}^{-3})$ and the refined temperature $T^{FT}=\alpha^{FT}T_0^{FT}/\left(1+\alpha^{FT}\right)$ $(T_0^{FT}=\ 25219\,\text{K}\,[1])$ with the coherent density ρ^{FT} from Eq.(5)

T, K [7]	α^{FT}	$\delta_\alpha\%$	T^{FT}, K	$\delta_T\%$	$\rho^*(T)$, $\text{kg}\cdot\text{m}^{-3}$	ρ^{FT}, $\text{kg}\cdot\text{m}^{-3}$	$\delta_\rho\%$
2200	0.0768	-8.3	1799	-18	15745	16019	+1.7

2750	0.1185	-9.7	2673	-2.8	15369	15422	+0.0
3200	0.1562	-11	3406	+6.5	15061	14920	-0.9
3270(s)	0.1618	-12	3512(s)	+7.4	15013	14847	-1.1
3270(l)	0.1456	-16	3206(l)	-2.0	15013	15057	+0.3
3616	0.1724	-18	3708	+2.6	14777	14714	-0.4
4011	0.2037	-20	4268	+6.4	14506	14331	-1.2
4378	0.2327	-22	4760	+8.7	14255	13994	-1.8
4718	0.2583	-23	5176	+9.7	14023	13710	-2.2
5036	0.2814	-25	5538	+10	13805	13462	-2.5
5334	0.3025	-27	5857	+9.8	13602	13244	-2.6
5619	0.3215	-29	6135	+9.2	13407	13054	-2.6
5892	0.3378	-30	6368	+8.1	13220	12894	-2.5
6160	0.3526	-32	6574	+6.7	13037	12753	-2.2
6425	0.3672	-33	6774	+5.4	12855	12617	-1.9
6693	0.3813	-35	6962	+4.0	12672	12487	-1.5
6966	0.3946	-36	7136	+2.4	12485	12369	-0.9
7250	0.4092	-38	7324	+1.0	12291	12240	-0.4
7472(d)			7472	0.0	12139	12139	0.0

*) – since our purpose is reconcilability after FT-calibration of the metastable IEX-data [7], first of all, with the stable IEX-data [14] on density, we used Eq.(1.1) in which the original T [14] – values have been replaced by the possibly incoherent (Section 2) T [7] – values to obtain the quasi-experimental points $\rho^*(T)$ [14] for the further comparison with $\rho^{FT}\left(T^{FT}\right)$.

The convincing and explainable reduction of a cumulative uncertainty in a step-by-step manner of FT-calibration is observable in the set $\delta_\alpha \to \delta_T \to \delta_\rho$ where the latter becomes indeed comparable with the acceptable experimental level. To obtain $\alpha^{FT} = \alpha[7]\rho[7]/\rho_0^{FT}$, the only one input FT – parameter from Eq.(5): $\rho_0 = \rho_c/Z_c$ has been used. Another single input FT – parameter T_0 is necessary and enough in accordance with the scaling meaning of α^{FT} to synchronize IIEX-temperatures with densities.

We demonstrate in Fig. 4 *the contributions of irreversibility* (IIEX-IEX) in the reported data for Ta [7] to illustrate the apparent solution of the long-standing IEX- problem concerning the too high heat capacity near T_m – point [9,10]. The comparison is performed at the equal FT-calibrated temperatures T^{FT} from Table 7. The meaningful value of FT – calibration becomes also clear from the much more pronounced shapes of polytropic enthalpy $h^{FT}(T) = h_P[7]\rho[7]/\rho_0^{FT}$ – and electrical resistivity $\rho_e^{FT}(T) = \rho_e[7]\rho_0/\rho_0^{FT}$ – dependences at the higher

temperatures $T > T_b^{\mathrm{Ta}} = 5731\,\mathrm{K}$. The proposed here *second*, in fact, FT – calibration takes into account that the standard for electrical IIEX-resistivity first $\rho_e(T)$ correction for thermal expansion was already introduced by the multiplier: $\rho(T)/\rho_0$[7]. There are two evident distinctive $T-$ stages of FT-calibrated C^{FT} in

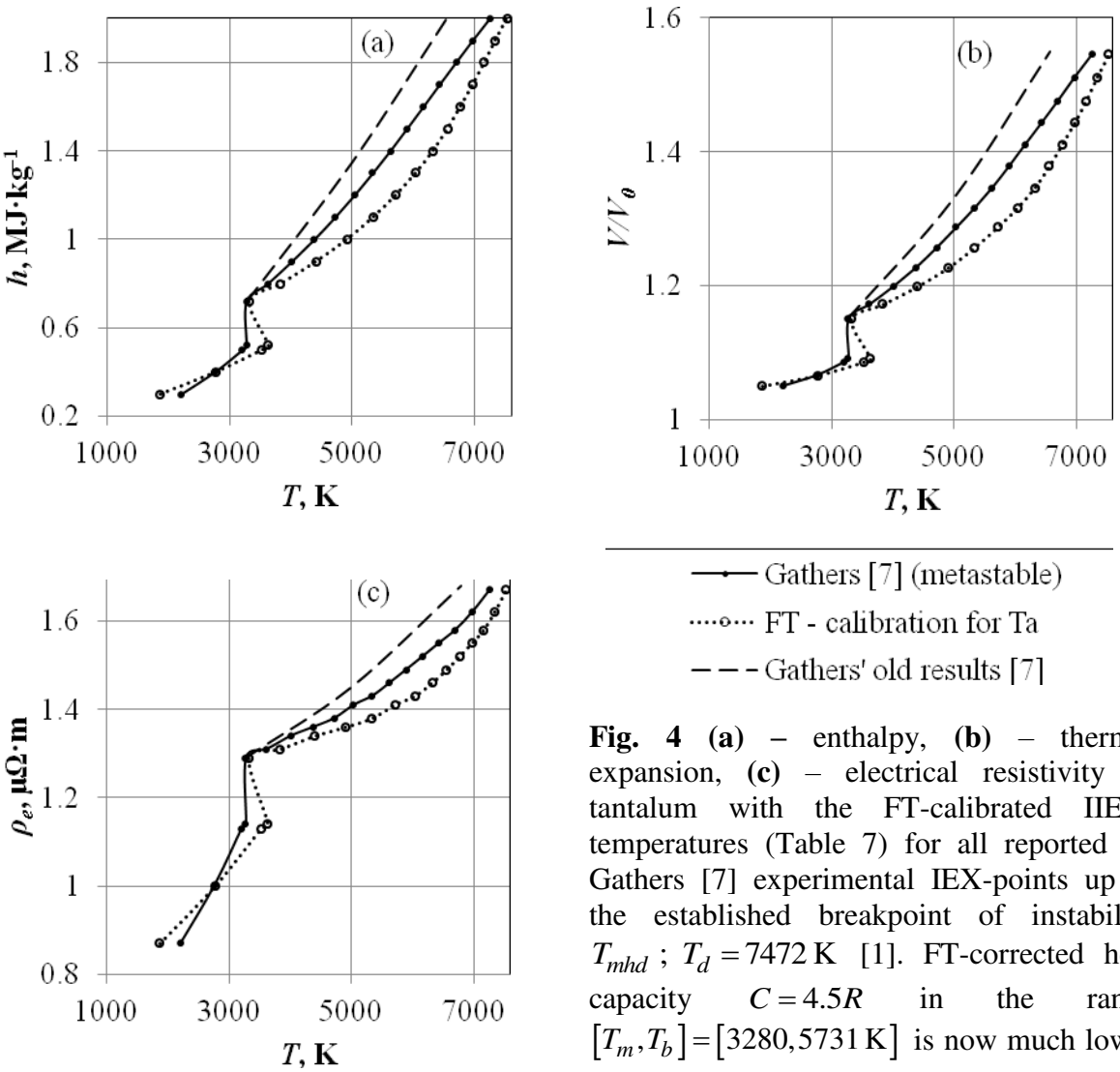

Fig. 4 (a) – enthalpy, **(b)** – thermal expansion, **(c)** – electrical resistivity of tantalum with the FT-calibrated IIEX-temperatures (Table 7) for all reported by Gathers [7] experimental IEX-points up to the established breakpoint of instability T_{mhd} ; $T_d = 7472\,\mathrm{K}$ [1]. FT-corrected heat capacity $C = 4.5R$ in the range $[T_m, T_b] = [3280, 5731\,\mathrm{K}]$ is now much lower than those $C \approx 8.3R$ and $C \approx 6.3R$ in the original work [7]

Fig.4a-c: 1) the normal polytropic heat capacity $C^{FT} = dh^{FT}/dT-$ values and 2) the sharply augmented $C^{FT}(T)-$ values developing after the approximate threshold of boiling $T_b^{\mathrm{Ta}} = 5731\mathrm{K}$ achievable at any subcritical ambient pressures. The FT-calibrated growth of $C^{FT}(T)$ in the extremely wide range of *v*-interphase for Ta $(T_d - T_b)^{\mathrm{Ta}} = 1741\,\mathrm{K}$ predicts even the higher values of its rate for growth

$dC^{FT}/(T_d - T_b)$ than those fitted in [7]. The observable in Fig. 4c augmented increase of electrical resistivity is the only consequent effect of the developing structural hydrodynamic instability *but not its trigger in FT-calibration.*

4.2 FT-calibration of stable supercritical high-pressure $(P = 0.3\,\text{GPa})$ IEX-data for aluminum [8].

The task of FT – calibration is essentially simplified in this case (see Fig.5) due to the more appropriate choice in [8] of the enthalpy in a condensed matter as

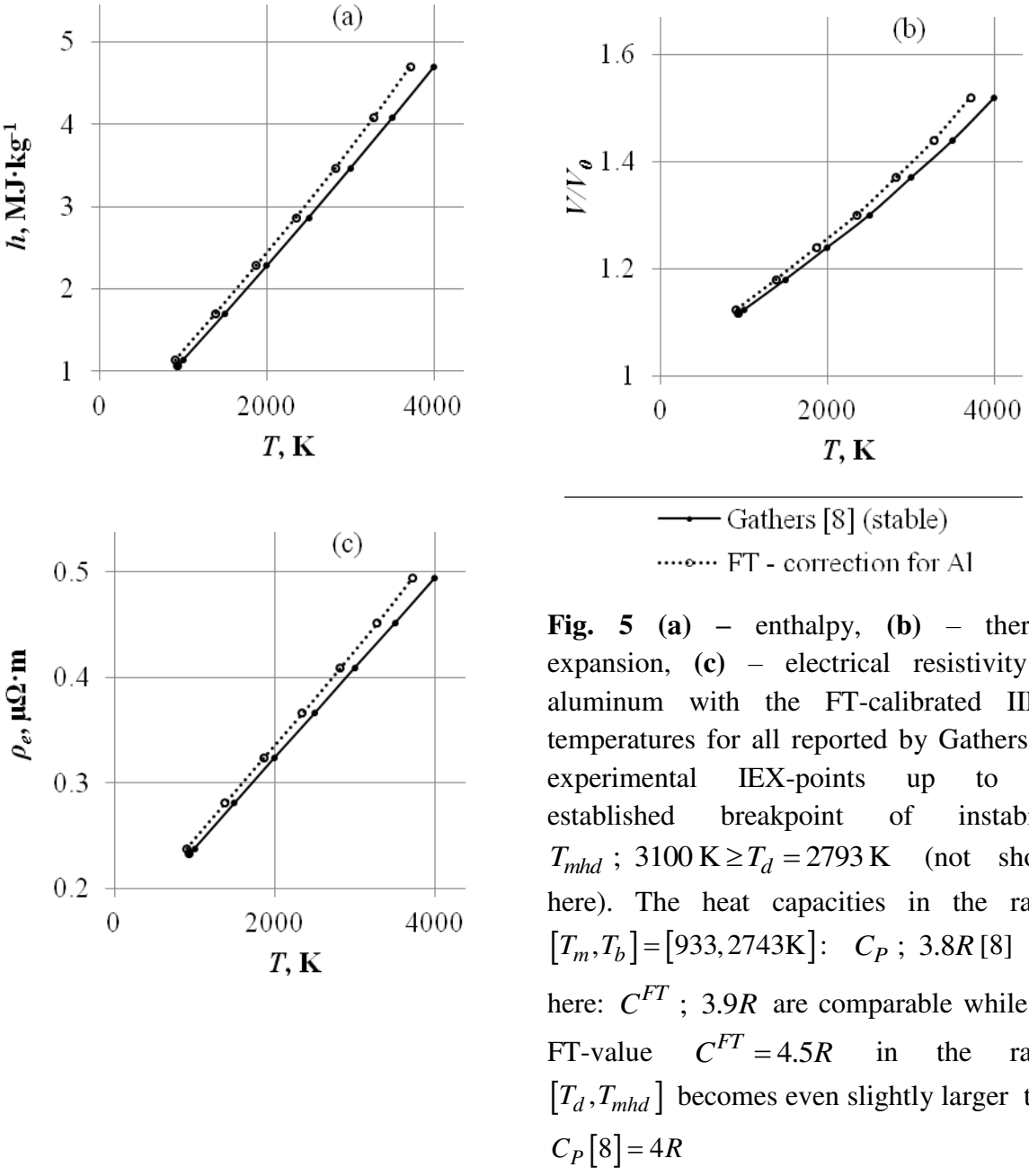

Fig. 5 (a) – enthalpy, **(b)** – thermal expansion, **(c)** – electrical resistivity of aluminum with the FT-calibrated IIEX-temperatures for all reported by Gathers [8] experimental IEX-points up to the established breakpoint of instability T_{mhd} ; $3100\,\text{K} \geq T_d = 2793\,\text{K}$ (not shown here). The heat capacities in the range $[T_m, T_b] = [933, 2743\text{K}]$: C_P ; $3.8R$ [8] and here: C^{FT} ; $3.9R$ are comparable while the FT-value $C^{FT} = 4.5R$ in the range $[T_d, T_{mhd}]$ becomes even slightly larger than $C_P[8] = 4R$

independent variable $h(\Delta t)$. Its linear polytropic change with temperature during

any experimental IIEX – shot implies the convenient system of linear relationships of the type those used in [11,12] for gold. However, it follows that the necessary for a stable supercritical condensed matter $\alpha[8]-$value is now a slightly complicated conversion multiplication $\alpha(T)=(T/v)dv/dT=(dv/dh)(Tdh/dT)/v$. In this case the elimination of IIEX-value $dh(t)=\delta h_{JL}$ (36[1]) requires its coherence with the ratio of both relative changes: dv/v and dT/T. The renewal CVL – diagram of Subsection 3.1 provides the reliable and inverse for Ta, inequality: $\alpha^{FT}>\alpha[8]$ for Al. It is the direct consiquence of a slightly higher location of supercritical IIEX- data $\rho[8]>\rho[13,15]$. As a result all FT-calibrated $T^{FT}-$ values are now decreased ($\delta_T\%<10\%$) in comparison with the reported $T[8]-$ data. The similar systematic shift of the FT-calibrated results for enthalpy and electrical resistivity shown in Fig. 5 become also recognizable.

5. Conclusions

1. The same predictive FT-model used earlier for ten alkali and alkaline-earth metals and recently for tantalum is applied to the soft metals: light aluminum and heavy gold with the purpose of a detailed critical point's and global *congruent vapor-liquid* phase diagram's renewal. The correspondence to the available static and dynamic experiments has been obtained.

2. To extend the conventional efforts of taking into account the many-particle cohesion with the local *electron density* on a single atom, the reduced *nucleon density* of mass m_n; M/N_A: $\omega_{nf}=\rho_{nf}/\rho_c\approx 10\pm 1$ spread within its effective spherical volume: $\pi\sigma_f^3/6$ has been defined. The slightly different $\sigma_f^{FT}-$ estimates in *f*-phases of element based exclusively on the FT- model's critical point parameters are reliably consistent with the tabular *covalent diameters* of Al, Au, Ta but not with the larger *atomic or vdW-diameters* usable in MD- simulations.

3. The proposed critical-point-dependent binding energy of elements is very large for light metals (Li, Be, Al) and significantly smaller for heavy metals (Ta,

Rb, Cs, Au). It is proportional to the FT-force: $\varepsilon^{FT}/\sigma_f^{FT}$ between the neighbor atoms acting on their nucleon mass m_n where the effective FT- well-depth: $\varepsilon^{FT}(T_c, Z_c)$ is the factor strongly different in metals, semiconductors and dielectrics, including molecular compounds.

4. The well-established earlier principle of global fluid asymmetry and its non-mean-field CVL-diagram provide the alternative to the concept of spinodal decay structural insight into the possible mechanism of the *mhd*-instability observable in the wide set of subsecond IEX-experiments.

5. The steady thermo-caloric heterogeneous structure of *v*-interphase revealed by FT-model in the nano-scales of observation is the supposed "driven force" for *mhd*- instability in a condensed matter of a measurable sample.

6. The natural and simple FT-calibration of IEX-data is proposed and tested on Ta and Al to exclude the assumed contribution of irreversibility in the respective temperature $T(t)-$ estimates and to consist the results of different laboratories for the non-isobaric polytropic processes of subsecond measurements.

7. The additional and rather challenging further research of the hypothesized different "wet" and "dry" shapes of $(T,s)-$diagram for light and heavy metals seems to be the promising option of the FT-model usage.

6. Declarations

The authors did not receive support from any organization for the submitted work.

The authors have no relevant financial or non-financial interests to disclose.

References

[1] G.S. Dragan, V.B. Rogankov, O.V. Rogankov, Int. J. Thermophys. (2022) 43:94. https://doi.org/10.1007/s10765-022-03018-9

[2] O.V. Rogankov, V.A. Mazur, V.B. Rogankov Fluid Phase Equil. 455(2018)15-23.

[3] O.V. Rogankov, V.A. Mazur, M.V. Shvets, V.B. Rogankov Fluid Phase Equil. 466(2018)79-88

[4] V.B. Rogankov, M.V. Shvets, O.V. Rogankov Fluid Phase Equil. 485(2019)101-110

[5] O.V. Rogankov, V.B. Rogankov Fluid Phase Equil. 529(2020)112843

[6] V.B. Rogankov, High Temperatues 47(2009)656-663

[7] G.R. Gathers, Int. J. Thermophys. 4(1983)149-156

[8] G.R. Gathers, Int. J. Thermophys. 4(1983)209-226

[9] G.R. Gathers, Int. J. Thermophys. 11(1990)693-708

[10] A. Cezairlian, G.R. Gathers, A.M. Malvezzi, A.P. Miiller, F. Righini, J.W. Shaner, Int. J. Thermophys. 11(1990)819-833

[11] E. Kaschnitz, G. Nussbaumer, G. Pottlacher, H. Jager, Int. J. Thermophys. 14(1993)251-257

[12] K. Boboridis, G. Pottlacher, H. Jager. Int. J. Thermophys. 20(1999)1289-1297

[13] M. Leitner, T. Leitner, A. Schmon, K. Aziz, G. Pottlacher. Metallurg. Mater. Transact. A 48 (2017) 3159.

[14] M.Leitner, W. Schroer, G. Pottlacher, Int. J. Thermophys (2018) 39:124 https://doi.org/10.1007/s10765-018-2439-3

[15] M.J.Assael, K. Kakosimos, R.M. Banish, J. Brillo, I. Egry, R. Brooks, P.N. Qested, K.C. Mills, A. Nagashima, Y. Sato, W.A. Wakeham, J. Phys. Chem, Ref. Data 35(2006)285-300.

[16] M.M. Martynyuk, Int. J. Thermophys. 14 (1993) 457-470.

[17] A.D. Rakhel. Int. J. Thermophys. 17 (1996) 1011-1024.

[18] S.N. Luo, T.J. Ahrens, T. Cagin, A. Strachan, W.A. Goddard III, D.C. Swift, Phys. Rev. B68(2003)134206

[19] L.M.N.B.F. Santos, J.N. Canongia Lopes, J.A.P. Coutinho, J.M.S.S. Esperanca, L.R. Gomes, I.M. Marrucho, L.P.N. Rebelo, J. Am. Chem. Soc. 129(2007)284-285

[20] C. Cadena, Q. Zhao, R.Q. Snurr, E.J. Maginn, J. Phys. Chem. B.110(2006)2821-2832

[21] G. Kaptay, Mater. Sci. Eng. A495(2008)19-26

[22] V. Morel, A. Bultel, B.G. Cheron, Int. J. Thermophys, 30(2009)1853-1863

[23] W.G. Hoover, G. Stell, E. Goldmark, G.D. Degani, J. Chem. Phys, 63(1975)5434-5438

[24] D.A. Young, A soft-sphere model for liquid metals, Lawrence Livermore Lab. 1977, 1-15

[25] V.I. Nedostup, High. Temp. 51(2013)72-78

[26] M.C. Kutney, M.T. Reagan, K.A. Smith, J.W. Teester, D.R. Herschbach, J. Phys. Chem. B104(2000)9513-9525

[27] I.C. Sanchez, S. O'Keefe, J.F. Xu, J. Phys. Chem. B120(2016)3705-3712

[28] C. Degranges, A. Margo, J. Delhommelle, Chem. Phys. Lett. 658(2016)37-42

[29] E. M. Apfelbaum, V. S. Vorob'ev. Int. J. Thermophys. 41:8. (2020) 1-14

[30] M.H. Abbasi, S. Blairs, Phys. Chem. Liq. 25(1993)201-204

[31] S. Blairs, M.H. Abbasi, J. Colloid Interface Sci, 304(2006)549-553

[32] Y. Zhang, J.R.G. Evans, S. Yang, J. Chem. Eng. Data, 56(2011)328-337

[33] B. Poling, J. Prausnitz, J. O'Connel, The properties of gases and liquids, Mc Graw-Hill Professional, 2000.